

Discretisation effects in the topological susceptibility in lattice QCD

A. Hart¹

(UKQCD and QCDSF Collaborations)

¹*School of Physics, University of Edinburgh, King's Buildings, Edinburgh EH9 3JZ, U.K.*

We study the topological susceptibility, χ , in QCD with two quark flavours using lattice field configurations that have been produced with an $\mathcal{O}(a)$ -improved clover quark action. We find clear evidence for the expected suppression at small quark mass, m_q , and examine the variation of χ with this mass and the lattice spacing, a . A joint continuum and chiral extrapolation yields good agreement with theoretical expectations as $a, m_q \rightarrow 0$. A moderate increase in autocorrelation is observed on the more chiral ensembles, but within large statistical errors. Finite volume effects are negligible for Leutwyler–Smilga parameter $x_{\text{LS}} \gtrsim 10$, and no evidence for a nearby phase transition is observed.

PACS numbers: 11.15.Ha, 12.38.Gc

I. INTRODUCTION

QCD is distinguished from the constituent quark models of hadronic physics by the presence of light sea quarks in the vacuum and one of the principal goals of lattice field theory is to provide an accurate theoretical description of their effects.

The topological charge, Q , and its associated susceptibility, χ , are especially sensitive to the presence and properties of the sea quarks. Chiral perturbation theory describes their variation with the quark mass, m_q . By comparing lattice Monte Carlo measurements with this expectation, we may understand how near we are to achieving the above aim.

Initial work on unimproved sea quark formulations (Wilson [1] and staggered [2, 3, 4, 5, 6, 7]) showed only weak evidence for the expected chiral ($m_q \rightarrow 0$) suppression of χ relative to the quenched ($m_q \rightarrow \infty$) theory at an equivalent lattice spacing, a (see [8, 9, 10] for reviews). A clearer chiral reduction was seen for improved fermion formulations, probably as a result of better chiral symmetry at finite lattice spacing [7]. $\mathcal{O}(a)$ -improved Sheikholeslami–Wohlert (SW, or “clover”) Wilson fermions showed a strong sea quark effect in a study at quasi-fixed lattice spacing, $a \simeq 0.1$ fm [8, 9, 11, 12, 13, 14]; mean field improved SW quarks also showed an effect [15]. Improved staggered fermion studies have also shown clear suppression of χ over a range of lattice spacings $0.09 \lesssim a \lesssim 0.12$ fm [7, 16, 17]. Studies using lattice sea quark formulations with chiral properties more comparable to those of the continuum have so far been limited to two dimensional models [18].

In the light of the improved staggered results, it is interesting to examine the effects of finite lattice spacing on the topological susceptibility from $\mathcal{O}(a)$ -improved SW quarks. This is useful not only from the theoretical viewpoint, but also when comparing the relative costs of producing independent field configurations in Monte Carlo simulations (the topological modes are expected to be amongst the slowest to decorrelate).

In this paper we extend the analysis of two flavour

$\mathcal{O}(a)$ -improved SW results at $a \simeq 0.1$ fm (included in this work with due acknowledgment) to cover a comparable range of lattice spacings to the improved staggered fermion study, using lattice QCD ensembles produced by the UKQCD and QCDSF collaborations. Moving to small quark masses (the lightest yet produced for Wilson-like fermions), we find strong evidence for the chiral suppression of χ . Finite volume effects are shown to be under control, and no strong autocorrelation is seen for the topological charge. We perform a joint continuum chiral and continuum extrapolation, and find good agreement with theoretical expectations.

The structure of this paper is as follows: in Section II we review the theoretical expectations for the chiral variation of the topological susceptibility in the continuum and on the lattice. We describe our measurements in Section III, and discuss their variation with m_q , a and the lattice volume. We conclude with a discussion in Section IV.

II. THE TOPOLOGICAL SUSCEPTIBILITY

Four-dimensional, Euclidean gauge fields can be classified by an integer-valued topological charge,

$$Q = \int d^4x \frac{1}{2} \varepsilon_{\mu\nu\sigma\tau} F_{\mu\nu}(x) F_{\sigma\tau}(x) \in \mathbb{Z}. \quad (1)$$

In the absence of a θ -term, $\langle Q \rangle = 0$ and the topological susceptibility, $\chi = \langle Q^2 \rangle / V$, has a finite, non-zero limit as the volume $V \rightarrow \infty$.

As the mass of the sea quarks is reduced the topological susceptibility is suppressed, the leading order behaviour being [19, 20, 21]

$$\chi(m_\pi^2) = \frac{(f_\pi m_\pi)^2}{4} \quad (2)$$

for two degenerate flavours, with corrections at $\mathcal{O}(m_\pi^4)$. This relation should hold when V is large enough that chiral symmetry is not restored, i.e.

$$x_{\text{LS}} \equiv m_q \Sigma V \simeq (f_\pi m_\pi)^2 V \gg 1, \quad (3)$$

TABLE I: The ensembles including the volume L^3T in lattice units, the number of configurations analysed, their separation in HMC trajectories, physical parameters and various measures of the physical volume.

label	β	κ_s	L^3T	$N_{\text{conf, sepn}}$	r_0	$(r_0 m_\pi)^2$	L/r_0	Lm_π	x_{LS}
q_1	5.20	0.13420	$16^3 32$	514, 10	4.077 (31)	5.67 (7)	3.9	9.3	150
u_2	5.20	0.13500	$16^3 32$	789, 10	4.754 (40)	3.87 (5)	3.4	6.6	55
u_3	5.20	0.13550	$16^3 32$	830, 10	5.041 (40)	2.15 (3)	3.2	4.6	24
u_4	5.20	0.13565	$16^3 32$	280, 10	5.246 (51)	1.67 (4)	3.0	3.9	16
u_5	5.20	0.13580	$16^3 32$	279, 10	5.320 (50)	1.22 (4)	3.0	3.3	11
q_6	5.25	0.13460	$16^3 32$	194, 10	4.737 (21)	5.44 (4)	3.4	7.9	79
u_7	5.25	0.13520	$16^3 32$	822, 10	5.138 (45)	3.90 (5)	3.1	6.1	41
q_8	5.25	0.13575	$24^3 48$	91, 10	5.430 (60)	1.99 (4)	4.4	6.2	85
u_9	5.26	0.13450	$16^3 32$	415, 10	4.708 (52)	5.73 (9)	3.4	8.1	85
u_{10}	5.29	0.13400	$16^3 32$	397, 10	4.813 (45)	7.70 (11)	3.3	9.2	105
q_{11}	5.29	0.13500	$16^3 32$	587, 5	5.227 (37)	4.84 (5)	3.1	6.7	47
q_{12}	5.29	0.13550	$12^3 32$	834, 5	5.756 (33)	3.53 (3)	2.1	3.9	10
q_{13}	5.29	0.13550	$16^3 32$	911, 5	5.560 (30)	3.30 (3)	2.9	5.2	25
q_{14}	5.29	0.13550	$24^3 48$	405, 5	5.566 (20)	3.30 (2)	4.3	7.8	127
q_{15}	5.40	0.13500	$24^3 48$	653, 2	6.088 (32)	6.03 (5)	3.9	9.7	162

where Σ is the chiral condensate [21] [38].

As $m_q \rightarrow \infty$, χ approaches the (constant) quenched value, $\chi^{(\text{qu})}$, from below. Higher order corrections to Eqn. (2) thus introduce a negative curvature at some intermediate quark mass. Various interpolating ansätze between the chiral and quenched regimes have been proposed [8, 10, 21]. In this paper we shall focus on one particular form, the large- N_c form [21], as motivated for SU(3) by Dürr [10]:

$$r_0^4 \chi = \frac{c_3 c_0 (r_0 m_\pi)^2}{c_3 + c_0 (r_0 m_\pi)^2} \quad \text{with} \quad c_0 = (r_0 f_\pi)^2 / 4, \quad (4)$$

$$c_3 = r_0^4 \chi^{(\text{qu})}.$$

Assuming the physical values of $r_0 = 0.5$ fm [22] and $f_\pi = 93$ MeV, then $c_0 = 0.0139$. This formula has been seen to work well in QCD [8, 9, 10] at fixed lattice spacing.

A. Lattice QCD

Eqn. (2) also holds for lattice QCD at finite lattice spacing for fermions with sufficiently good chiral properties [23, 24]. In general, however, the lattice topological susceptibility is related to the continuum by additive and multiplicative renormalisation factors, Z and M :

$$r_0^4 \chi^{(\text{lat})} = Z^2 r_0^4 \chi^{(\text{cont})} + M. \quad (5)$$

These competing factors are in general functions of the lattice spacing and the quark mass (partly implicitly

through the coupling, g^2). The upshot of this is that discretisation effects act to reduce χ below its continuum limit at large m_q , but to increase it in the chiral limit. A recent discussion can be found in [17]. Formally, before examining the sea quark mass dependence, we should first perform a continuum extrapolation of χ at fixed m_q to remove the effect of these renormalisation factors. This is, however, not possible with the ensembles we have available (especially if we do not admit interpolation in m_q of measurements at finite a). To attempt a full analysis of our data we must assume that the continuum and chiral limits commute sufficiently well that we can either perform the $m_q \rightarrow 0$ limit first at fixed a , or that we can carry out a joint chiral and continuum extrapolation using a single formula.

The first approach was used in [8, 9], fitting Eqns. (2) and (4) to data at $a \simeq 0.1$ fm. Constraints of simulation mean that this study cannot contribute many ensembles at comparably light sea quark mass but different a . We cannot, therefore, extend the above method by carrying out chiral fits at other lattice spacings so we can look at discretisation effects in the fit parameters. Instead we follow the second approach. Allowing $c_{0,3}$ to have a leading order lattice spacing correction (quadratic for the lattice action considered here)

$$c_0(r_0) = c_{00} + \frac{c_{01}}{r_0^2}, \quad c_3(r_0) = c_{30} + \frac{c_{31}}{r_0^2}, \quad (6)$$

in Eqn. (4), we obtain:

$$r_0^4 \chi = \frac{c_{30} c_{00} (r_0 m_\pi)^2}{c_{30} + c_{00} (r_0 m_\pi)^2} + \frac{1}{r_0^2} \left(k_1 + \frac{(r_0 m_\pi)^2}{(c_{30} + c_{00} (r_0 m_\pi)^2)^2} (c_{01} c_{30}^2 + c_{31} c_{00}^2 (r_0 m_\pi)^2) \right). \quad (7)$$

We have added a general constant, $k_1 \geq 0$, to allow χ to have a non-zero chiral limit at finite lattice spacing, as might occur in the absence of exact zero modes in the lattice Dirac operator [8]. A check of our results is consistency of the fitted parameters with the results for $r_0 \simeq 5$ from [8, 9].

III. MEASUREMENTS

We have calculated the topological charge and susceptibility using ensembles generated by the UKQCD [13, 25, 26] and QCDSF [27, 28] collaborations. Details of these ensembles are given in Table I (taken in the main from [28]). The lattice spacings lie in the range $0.08 \lesssim a \lesssim 0.12$ fm. The SU(3) gauge fields are governed by the Wilson plaquette action, with two flavours of SW fermions. The improvement parameter, c_{sw} , has been chosen so that the leading order discretisation errors vary quadratically with the lattice spacing [29]. The exact Hybrid Monte Carlo (HMC) simulation algorithm is used, which avoids finite step-size errors.

We measure Q using the method of [8]: ten cooling sweeps are applied using the Wilson gauge action. The cooling action has relatively little effect on the topological susceptibility [17]. Ten cools strikes a good balance between adequate suppression of these ultraviolet dislocations and excessive destruction of the long range topological structure [8, 17]. The choice of operator does not matter in the continuum limit, at least for the quenched theory [30], and a reflection-symmetrised “twisted plaquette” lattice topological charge operator is used. In Fig. 1 we show the variation of the topological charge as a function of Monte Carlo simulation time for three ensembles over a range of sea quark mass. The histograms of Q (using unit width bins, although in the rest of the analysis the topological charge is not rounded to the nearest integer value) show good agreement with the expected Gaussian form. Although $\langle Q \rangle = 0$ within statistical errors, we opt (for consistency with earlier studies) to subtract terms in $\langle Q \rangle$ from χ . Both this and the choice of whether to round Q to integer values affect χ by much less than one standard deviation.

This algorithm for measuring χ has already been studied in the quenched theory (the Wilson gauge action), and continuum extrapolation yields $c_{30} = 0.065$ (3) and $c_{31} = -0.28$ (4) [9].

The decorrelation of Q is good (see Fig. 1, and [8, 9, 25] for details of some other ensembles). More quantitatively, we measure the integrated autocorrelation, $\tau_{\text{int}}(Q)$, using an implementation of the sliding window method

[31], with results shown in Table II (scaled to units of HMC trajectories) [39]. With the exceptions of ensembles $q_{8,12,15}$ and u_{10} , there is weak evidence for a slow increase in τ_{int} from $\mathcal{O}(10)$ HMC trajectories for the least chiral ensembles to $\mathcal{O}(30)$ trajectories for the most chiral. We plot these data for the $16^3 32$ ensembles in Fig. 2 (omitting the least chiral point). The trend is no stronger for any particular gauge coupling, β , but the statistical errors and available range of $(r_0 m_\pi)^2$ make definitive statements difficult. Of the outliers, we note that ensembles $q_{8,15}$ have only a limited number of trajectories and, as we discuss later, q_{12} is the smallest physical volume studied.

Barring these possible exceptions, we have confidence that the topological susceptibility may be estimated free from autocorrelation effects and the statistical errors quoted are from a jack-knife analysis using 10 bins. No increase in the statistical error estimates for χ was found with larger bins, as expected when comparing τ_{int} to the bin size. Results for the topological susceptibility are given in Table II and plotted against quark mass in Fig. 3.

A. Discretisation effects

There is a significant suppression of the topological susceptibility in the chiral limit. In Fig. 3 we show the leading order chiral expectation of Eqn. (2), using the physical value for f_π . There is approximate agreement

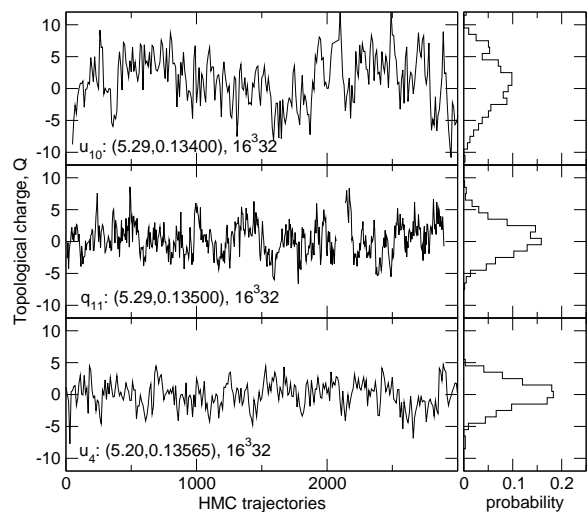


FIG. 1: Partial time histories for the topological charge for ensembles $u_{10,4}$ and q_{10} , with normalised histograms of the topological charge.

for $(r_0 m_\pi)^2 \lesssim 3$, although we note that discretisation effects tend to increase χ and exaggerate the range of agreement. We do not see clear evidence for χ deviating from a rapid decrease with m_q at finite lattice spacing as in [17], although critical slowing prevents exploration of sea quarks comparably light with those simulated in that study.

To quantify the effects of lattice artifacts, it is useful to consider χ over the full range of sea quark masses. Assuming that Eqn. (7) holds, we can use it to perform a chiral extrapolation of χ whilst allowing for (leading order) discretisation effects. We exclude ensemble u_{10} , whose statistical error is probably unreliable, and ensemble q_{12} which has a small volume (see on). Ensembles $q_{8,15}$ also have large autocorrelation, and we remark that excluding them from the fitted data had no statistically significant effect. We fit only the dynamical results, with the quenched parameters fixed. In principle we could avoid this and fit the quenched data as well, assigning all such points an arbitrarily large value of $(r_0 m_\pi)^2$. Such fits do not converge well, however. This was probably as a result of the data being arranged as two distinct clusters in $(r_0 m_\pi)^2$.

We show the fits to Eqn. (7) in Table III, with the $k_1 = 0$ results (Fit 1) plotted in Fig. 3 for a representative sample of lattice spacings, and in Fig. 4.

It is interesting to note that even for the heaviest sea quarks simulated, the discretisation effects act to increase χ . To see a crossover to the quenched behaviour (where a decrease is seen), the fits suggest we need $(r_0 m_\pi)^2 \gtrsim 25$. It is thus clear that for all the ensembles the vacuum has been qualitatively altered from that of the quenched theory by the presence of the sea quarks. As expected, topological degrees of freedom appear to be more sensitive to such changes than most hadronic observables.

TABLE II: The integrated autocorrelation estimates for the topological charge, and topological susceptibility.

label	τ_{int}	$r_0^4 \chi$
q_1	11 (2)	0.0494 (32)
u_2	16 (3)	0.0445 (30)
u_3	30 (13)	0.0310 (38)
u_4	26 (8)	0.0248 (28)
u_5	29 (15)	0.0230 (25)
q_6	12 (1)	0.0451 (32)
u_7	19 (4)	0.0392 (28)
q_8	92 (16)	0.0302 (68)
u_9	14 (4)	0.0433 (36)
u_{10}	125 (40)	0.0683 (68)
q_{11}	20 (6)	0.0369 (42)
q_{12}	78 (35)	0.0306 (52)
q_{13}	22 (8)	0.0276 (33)
q_{14}	25 (15)	0.0356 (57)
q_{15}	150 (22)	0.0325 (87)

TABLE III: Fits to Eqn. (7). Numbers in italic face were fixed in the fit. Fit 2 was carried out with two different sets of initial values, as described in the text.

parameter	Fit 1	Fit 2	
c_{00}	0.0135 (26)	0.0036 (30)	0.0283 (36)
c_{01}	0.2595 (229)	0.1074 (250)	1.453 (522)
c_{30}	<i>0.065</i>	<i>0.065</i>	<i>0.065</i>
c_{31}	<i>-0.28</i>	<i>-0.28</i>	<i>-0.28</i>
k_1	<i>0</i>	0.0149 (51)	-0.028 (9)
$\chi^2/\text{d.o.f.}$	1.043	0.980	0.721

For $r_0 = 5.0 \pm 0.2$ (the range studied in [8, 9]), these fits suggest $c_0 = 0.024$ (3)(1)(1), where the errors arise from those on c_{00} , c_{01} and the above range of r_0 respectively. This figure agrees very closely with $c_0 = 0.22$ (7) obtained in the previous work for Eqn. (4), and gives confidence in the consistency of our fits.

In addition to the errors arising from the statistical variation in the data, there is also a systematic error arising from the uncertainty in the quenched behaviour. We attempt to account for this by repeating the fits with c_{30} and c_{31} varying by one standard deviation in each direction: c_{00} varies by ± 0.003 under this, and it is clear that this is a sub-leading effect that can be ignored.

The fitted $c_{00} = 0.0135$ (26) corresponds to $f_\pi = 91.6$ (8.8) MeV. This agrees surprisingly well both with the experimental (and 2+1-flavour) QCD measurement (93 MeV) and measurements by other methods on $N_f = 2$ SW actions ($\simeq 97.0$ (0.3) MeV in these conventions, rescaled from [32]). The leading order lattice spacing correction to this increases f_π , as expected. The size of this correction is consistent with those obtained

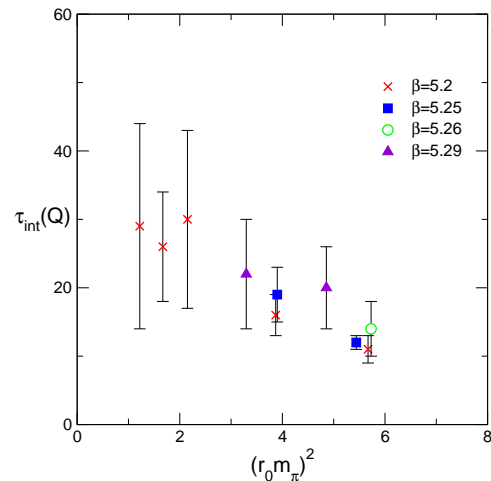


FIG. 2: Integrated autocorrelation estimates for topological charge on the $16^3 32$ lattice volumes, labeled by gauge coupling, β .

for other methods (see Fig. 35 of [32], for instance, although the different gauge actions and operators will, of course, lead to different lattice artifacts).

It is useful here to consider whether there is any evidence for χ having a non-zero chiral limit at finite a . In Fit 2 of Table III we show the result lifting the restriction $k_1 = 0$. The fits are extremely unstable; the first column is the result of starting with all free parameters being zero, whilst the second takes the results of Fit 1 as the initial values. This instability probably arises from the most chiral data points being clustered around $r_0 = 5$. We conclude that whilst we cannot rule out a non-zero chiral limit, the data appears to be described more consistently when such a term is not present. For the remainder of the paper we therefore concentrate on the results from Fit 1.

B. Finite volume effects

In [17] the lattice volumes were sufficiently large that the topological charge on subvolumes (of size L^4) varied independently; indeed a reduction in statistical error on χ was achieved by exploiting this self-averaging. We did not find the same in this study, and this prompts us to consider more carefully whether the topological susceptibility exhibits finite volume contamination.

In general we expect finite volume effects to lead to a reduction in χ : a small lattice excludes large instantons. In the quenched theory this restriction is negligible once $L/r_0 \gtrsim 2.5$ [33]. With dynamical sea quarks present, small volumes can, in addition, see a restoration of chiral symmetry with the leading order chiral variation now

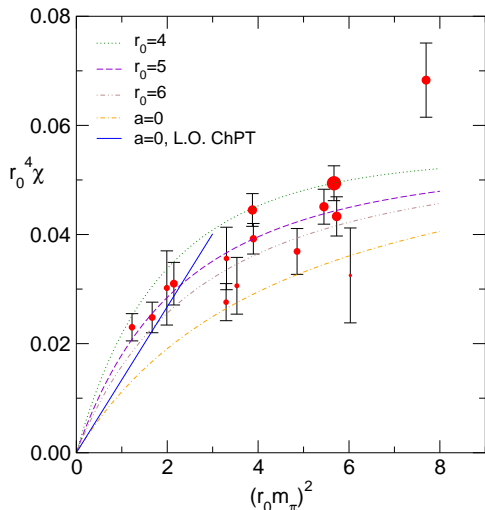


FIG. 3: The variation of the topological susceptibility. To guide the eye, the point size is proportional to r_0^{-2} . The single fitted curve Eqn. (7) is shown for the continuum limit and lattice spacings representative of the plotted data. The expectation from continuum chiral perturbation theory at leading order is also shown.

being $\chi \propto (m_q)^{N_f} \propto (m_\pi)^{2N_f}$. Avoiding this requires $x_{\text{LS}} \gg 1$, although the precise limit is not known. What is also not clear is how the behaviour interpolates between this and Eqn. (3) as we vary x_{LS} ; we do not address this in this study.

Finally, we need the lattice to be large in units of the pion correlation length, $Lm_\pi \gg 1$. Spectroscopy suggests $Lm_\pi \gtrsim 5.7$ is necessary to render the low-lying hadron states free of finite volume effects [34]. This limit is, however, associated more with pion exchange than phase structure and is probably unduly stringent for this study.

In Table I we show all three measures of FVEs. All the above limits seem well satisfied and we do not expect, or see, any sign of chiral symmetry restoration or significant finite volume effects. Certainly we do not see the smaller volumes lying consistently below the fitted curve.

The ensembles $q_{12,13,14}$ vary only in volume, and no strong suppression of χ is seen as V is reduced. Nonetheless, we choose to exclude q_{12} , the smallest lattice, from the scaling analysis as the volume is particularly small.

We can attempt to quantify the effects of finite volume by repeating the fit with $k_1 = 0$, progressively excluding the ensembles with the smallest x_{LS} (u_5, u_4, \dots) until the fits become unreliable. The fit parameters remained consistent within statistical errors. We conclude that finite volume effects are not significant at this level of statistical accuracy if $x_{\text{LS}} \gtrsim 10$.

IV. SUMMARY

We have carried out a systematic study of the topological susceptibility, χ , in lattice QCD with two light quark flavours over a range of lattice spacings and sea quark masses using ensembles generated by the UKQCD and QCDSF collaborations. We find compelling evidence for suppression of χ with decreasing quark mass. Finite

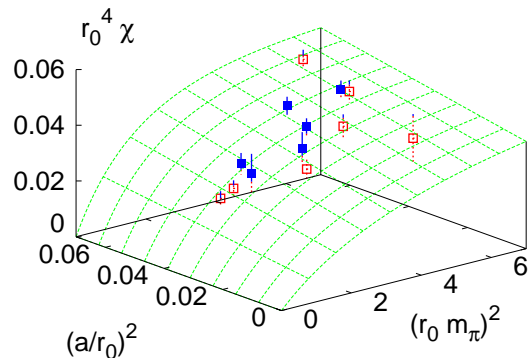


FIG. 4: Combined chiral and continuum extrapolation of the topological susceptibility. Solid (blue) points and error bars denote data points lying above the fitted surface. Open (red) points and dashed error bars denote data points lying below.

volume contamination of the results was not seen, and $x_{\text{LS}} \gtrsim 10$ is necessary to avoid such effects on the topological degrees of freedom.

We observe a slight (and, in truth, statistically insignificant) increase in the integrated autocorrelation of the topological charge, Q , as the sea quark mass is reduced, although this effect is not marked despite a critical slowing of the HMC algorithm [25, 26]. The autocorrelation times are, in general, small enough not to bias the jack-knife estimates of the statistical errors on our data.

There have been suggestions that at $\beta \simeq 5.2$ the $N_f = 2$ $\mathcal{O}(a)$ -improved SW action exhibits evidence for a nearby phase transition [14, 35, 36]. This transition affects most strongly observables with the quantum numbers of the vacuum, and we do not expect (or find) a strong effect on the topological susceptibility. It may, however, induce additional mass dependence in r_0 [36], although we see no signal in $r_0^4 \chi$ (whose fourth power would presumably magnify any such effect, distorting the data away from Eqn. (7)). It may also lead to large autocorrelation [36]. Whilst a large integrated autocorrelation is seen for one ensemble at large sea quark mass, this is at $\beta = 5.29$ which does not immediately fit the hypothesis of [36]. No unexpected trends were seen for $\beta = 5.2$.

The chiral variation of the data was compared to a theoretically motivated ansatz for the behaviour of χ over the full range of sea quark masses. This was extended to allow for variation of χ with the lattice spacing, and a joint chiral/continuum extrapolation was carried out for $0.08 \lesssim a \lesssim 0.12$ fm (over a factor of 2 in a^2). The behaviour was as expected: the continuum limit of

$f_\pi = 91.6$ (8.8) MeV was remarkably consistent with physical expectations, with discretisation effects tending to increase its value (as seen in other determinations [37]).

The discretisation effects tended to increase the topological susceptibility on all the ensembles. This agrees with expectations for the chiral limit and is in contrast to the quenched theory, where they suppress χ . This suggests that, relative to the quenched theory, there are fundamental differences in the vacuum due to sea quarks, even for the largest m_q . The topological susceptibility is more sensitive to these differences than, for example, most quantities in the light hadron spectrum.

In summary, the topological susceptibility is a sensitive probe of the vacuum and chiral properties of the lattice action. Although the $\mathcal{O}(a)$ -improved SW action formally breaks the chiral symmetry at finite lattice spacing, the behaviour of χ suggests that the effects are not significant at the lattice spacings simulated. The chiral behaviour of this action is comparably good to that of other actions currently used in large-scale simulations, and makes it a suitable laboratory for studying topologically sensitive states, including the η' meson.

Acknowledgments

The author is grateful to G. Schierholz and M. Teper for useful discussions; to D. Hepburn, A.C. Irving and D. Pleiter for providing estimates of quantities for ensembles u_5 and q_{15} in Table I; and to the Royal Society for financial support.

-
- [1] T χ L, G. S. Bali *et al.*, Phys. Rev. **D64**, 054502 (2001), [hep-lat/0102002].
- [2] K. M. Bitar *et al.*, Phys. Rev. **D44**, 2090 (1991).
- [3] Y. Kuramashi, M. Fukugita, H. Mino, M. Okawa and A. Ukawa, Nucl. Phys. Proc. Suppl. **26**, 275 (1992).
- [4] Y. Kuramashi, M. Fukugita, H. Mino, M. Okawa and A. Ukawa, Phys. Lett. **B313**, 425 (1993).
- [5] B. Alles, M. D'Elia and A. Di Giacomo, Nucl. Phys. Proc. Suppl. **83**, 431 (2000), [hep-lat/9912012].
- [6] B. Alles, M. D'Elia and A. Di Giacomo, Phys. Lett. **B483**, 139 (2000), [hep-lat/0004020].
- [7] A. Hasenfratz, Phys. Rev. **D64**, 074503 (2001), [hep-lat/0104015].
- [8] UKQCD, A. Hart and M. Teper, hep-ph/0004180.
- [9] UKQCD, A. Hart and M. Teper, Phys. Lett. **B523**, 280 (2001), [hep-lat/0108006].
- [10] S. Dürr, Nucl. Phys. **B611**, 281 (2001), [hep-lat/0103011].
- [11] UKQCD, A. Hart and M. Teper, Nucl. Phys. Proc. Suppl. **83**, 476 (2000), [hep-lat/9909072].
- [12] UKQCD, A. Hart and M. Teper, hep-lat/0009008.
- [13] UKQCD, C. R. Allton *et al.*, Phys. Rev. **D65**, 054502 (2002), [hep-lat/0107021].
- [14] UKQCD, A. Hart, Nucl. Phys. Proc. Suppl. **106**, 575 (2002), [hep-lat/0110167].
- [15] CP-PACS, A. Ali Khan *et al.*, Phys. Rev. **D64**, 114501 (2001), [hep-lat/0106010].
- [16] MILC, C. Bernard *et al.*, Nucl. Phys. Proc. Suppl. **119**, 991 (2003), [hep-lat/0209050].
- [17] C. Bernard *et al.*, Phys. Rev. **D68**, 114501 (2003), [hep-lat/0308019].
- [18] S. Dürr and C. Hoelbling, hep-lat/0311002.
- [19] R. J. Crewther, Phys. Lett. **B70**, 349 (1977).
- [20] P. Di Vecchia and G. Veneziano, Nucl. Phys. **B171**, 253 (1980).
- [21] H. Leutwyler and A. Smilga, Phys. Rev. **D46**, 5607 (1992).
- [22] R. Sommer, Nucl. Phys. **B411**, 839 (1994), [hep-lat/9310022].
- [23] S. Chandrasekharan, Phys. Rev. **D60**, 074503 (1999), [hep-lat/9805015].
- [24] L. Giusti, G. C. Rossi, M. Testa and G. Veneziano, Nucl. Phys. **B628**, 234 (2002), [hep-lat/0108009].
- [25] UKQCD, C. Allton *et al.*, in preparation (2003).
- [26] UKQCD, A. C. Irving, Nucl. Phys. Proc. Suppl. **119**, 341 (2003), [hep-lat/0208065].
- [27] QCDSF-UKQCD, S. Booth *et al.*, Phys. Lett. **B519**, 229 (2001), [hep-lat/0103023].

- [28] A. A. Khan *et al.*, hep-lat/0312030.
- [29] ALPHA, K. Jansen and R. Sommer, Nucl. Phys. **B530**, 185 (1998), [hep-lat/9803017].
- [30] M. Teper, Nucl. Phys. Proc. Suppl. **83**, 146 (2000), [hep-lat/9909124].
- [31] N. Madras and A. D. Sokal, J. Statist. Phys. **50**, 109 (1988).
- [32] JLQCD, S. Aoki *et al.*, Phys. Rev. **D68**, 054502 (2003), [hep-lat/0212039].
- [33] B. Lucini and M. Teper, JHEP **06**, 050 (2001), [hep-lat/0103027].
- [34] UKQCD, C. R. Allton *et al.*, Phys. Rev. **D60**, 034507 (1999), [hep-lat/9808016].
- [35] UKQCD, A. Hart and M. Teper, Phys. Rev. **D65**, 034502 (2002), [hep-lat/0108022].
- [36] ALPHA, R. Sommer *et al.*, hep-lat/0309171.
- [37] CP-PACS, A. Ali Khan *et al.*, Phys. Rev. **D65**, 054505 (2002), [hep-lat/0105015].
- [38] By the “pion” we mean the lightest pseudoscalar meson with valence quarks of the same mass as the two degenerate sea quarks flavours. The PCAC relation predicts $m_q \propto m_\pi^2$ and we shall use the latter as a measure of the quark mass.
- [39] Autocorrelations are notoriously hard to estimate in realistic ensembles, and for consistency of analysis here there are slight differences from earlier studies of the intermediate quark mass ensembles [8, 9]. With this in mind, the results presented here have been compared to those from a number of other algorithms for determining τ_{int} , and show a good degree of robustness.